Magnetic Resonance in Medicine 59:423–429 (2008)

Quantification of Hepatic Transaldolase Exchange Activity and Its Effects on Tracer Measurements of Indirect Pathway Flux in Humans

John G. Jones,[1]* Paula Garcia,[2] Cristina Barosa,[1] Teresa C. Delgado,[1] M. Madalena Caldeira,[3] and Luisa Diogo[2]

Exchange of hepatic glucose-6-phosphate (G6P) and glyceraldehyde-3-phosphate via transaldolase modifies hepatic G6P enrichment from glucose or gluconeogenic tracers. Transaldolase exchange was quantified in five healthy, fed subjects following an oral bolus of [1,2,3-$^{13}C_3$]glycerol (25–30 mg/kg) and paracetamol (10–12 mg/kg). ^{13}C Isotopomers of hepatic G6P were quantified by ^{13}C NMR spectroscopy of urinary glucuronide. [1,2,3-$^{13}C_3$]- and [4,5,6-$^{13}C_3$]glucuronide isotopomers, representing the conversion of [1,2,3-$^{13}C_3$]glycerol to G6P via dihydroxyacetone phosphate, were resolved from [1,2-$^{13}C_2$]- and [5,6-$^{13}C_2$]glucuronide ^{13}C-isotopomers, derived from metabolism of [1,2,3-$^{13}C_3$]glycerol via pyruvate and phosphoenolpyruvate. Enrichment of [1,2,3-$^{13}C_3$]glucuronide was significantly less than that of [4,5,6-$^{13}C_3$]glucuronide (1.30 ± 0.57% versus 1.67 ± 0.42%, $P < 0.05$). Also, [1,2-$^{13}C_2$]glucuronide enrichment was significantly less than that of [5,6-$^{13}C_2$]glucuronide (0.28 ± 0.08% versus 0.36 ± 0.03%, $P < 0.05$). Transaldolase and triose phosphate isomerase exchange activities were estimated by applying the ^{13}C-isotopomer data to a model of hepatic sugar phosphate metabolism. Triose phosphate isomerase exchange was ≈99% complete and did not contribute significantly to the unequal ^{13}C-isotopomer distributions of the glucuronide triose halves. Instead, this was attributable to 25 ± 23% of hepatic G6P flux undergoing transaldolase exchange. This results in substantial overestimates of indirect pathway contributions to hepatic glycogen synthesis with tracers such as [5-^{3}H]glucose and $^{2}H_2O$. Magn Reson Med 59:423–429, 2008. © 2008 Wiley-Liss, Inc.

Key words: indirect pathway; transaldolase; gluconeogenesis; glycogen; triose phosphate isomerase

Hepatic glucose-6-phosphate (G6P) lies at the metabolic crossroads of hepatic glucose and glycogen metabolism. Under fasting conditions when the liver is a net producer of glucose, hepatic G6P is generated by the hydrolysis of glycogen and from gluconeogenesis and is then converted to glucose via G6P. Under fed conditions there is net hepatic glycogen synthesis from both glucose and from gluconeogenic precursors. These metabolic pathways converge at G6P and the hexose carbon skeletons are then incorporated into glycogen via glucose-1-phosphate and UDP-glucose. The gluconeogenic contribution to G6P synthesis is modified in a variety of human diseases, including insulin- and noninsulin-dependent diabetes, cirrhosis, and malaria (1–4). Therefore, quantifying the fraction of G6P derived from gluconeogenesis is a key parameter for defining hepatic carbohydrate metabolism under these and other pathophysiological conditions. In humans, several different tracer methods have been developed for quantifying the contribution of gluconeogenesis to hepatic G6P flux. Hepatic G6P enrichment from these tracers can be quantified noninvasively by analysis of urinary glucuronide enrichment (5–7).

Implicit in all measurements of hepatic gluconeogenesis using labeled gluconeogenic substrates is the assumption that G6P molecules derived from non-gluconeogenic precursors (i.e., glycogenolysis) are not labeled with the tracer.[1] Likewise, when labeled glucose is used to determine the contribution of direct and indirect pathways of hepatic glycogen synthesis under fed conditions, dilution of the glucose tracer at the level of hepatic G6P is assumed to be entirely due to gluconeogenic G6P production.

The possibility that transaldolase (TA) exchange could invalidate these assumptions was recognized by Landau and co-workers (8–10). TA catalyzes the exchange between the glyceraldehyde-3-phosphate (GA3P) moiety (i.e., carbons 4, 5, and 6) of fructose-6-phosphate (F6P) and free GA3P in many tissues (11–13). This exchange is independent of oxidative pentose phosphate pathway (PPP) flux, hence tissues that have relatively low oxidative PPP utilization of G6P, such as liver, may nevertheless have significant TA exchange activity (13). Since G6P and F6P are in rapid exchange, G6P molecules derived from glucose or glycogen are exposed to TA activity. With gluconeogenic tracers that label GA3P, the effect of TA exchange is to transfer the label to G6P molecules derived from glucose or glycogen. Hence, the gluconeogenic contribution is overestimated relative to the contribution from

[1]NMR Research Unit, Department of Biochemistry and Center for Neurosciences and Cell Biology, University of Coimbra, Portugal.

[2]Pediatrics Hospital of Coimbra, Portugal.

[3]Department of Chemistry, University of Coimbra, Portugal.

Grant sponsor: Portuguese Foundation of Science and Technology; Grant number: POCTI/QUI/55603/2004; Grant sponsor: Juvenile Diabetes Research Foundation International; Grant number: JDRFI 1-2006-74.

*Correspondence to: John G. Jones, DSc, NMR Research Unit, Center for Neurosciences and Cell Biology, Faculty of Sciences and Technology, University of Coimbra, 3004-401 Coimbra, Portugal. E-mail: jones@cnc.cj.uc.pt

Received 16 February 2007; revised 17 September 2007; accepted 25 September 2007.

DOI 10.1002/mrm.21451

Published online 8 January 2008 in Wiley InterScience (www.interscience.wiley.com).

[1]With $^{2}H_2O$, position 2 is enriched as a result of G6P-F6P exchange but the other sites are unlabeled.

glucose or glycogen. Under fed conditions, when the contribution of glucose via the direct pathway to G6P synthesis is quantified with a tracer such as [5-^{3}H]glucose, TA exchange depletes the amount of [5-^{3}H]G6P resulting in an underestimate of the direct pathway fraction and a corresponding overestimate of the gluconeogenic (indirect) pathway contribution to G6P flux (10).

The extent of TA activity in human liver during either the fed or fasting state is not known. We present new observations of glucuronide ^{13}C-isotopomer distributions that are best explained by the presence of TA exchange. We developed a metabolic model that relates the ^{13}C-isotopomer distributions of glucuronide to TA exchange. Following ingestion of [1,2,3-$^{13}C_3$]glycerol, human glucuronide ^{13}C-isotopomer distributions were quantified by ^{13}C NMR and the extent of TA exchange for the hepatic G6P pool was estimated. Our results indicate that a substantial fraction of hepatic G6P undergoes TA exchange in healthy, fed humans. Failure to account for this activity could result in a significant overestimation of the indirect pathway contribution to hepatic glycogen synthesis with some commonly used tracers of human hepatic carbohydrate metabolism.

MATERIALS AND METHODS

Human Studies

Human studies were performed according to study protocols approved by the Ethics Committees of the University and Pediatrics Hospitals of Coimbra after informed consent was obtained from the subjects. Five healthy nonobese subjects (1 male, 4 females; 20 ± 4 years; 53 ± 13 kg) were studied. After an overnight fast, at 08:00, 11:00, and 14:00 subjects ingested 1 g/kg body weight of cornstarch as an aqueous slurry. Paracetamol (10–12 mg/kg) was also ingested at 11:00 and the cornstarch meal at 14:00 was accompanied by phenylbutyric acid (5 mg/kg) and [1,2,3-$^{13}C_3$]glycerol (25–30 mg/kg). Blood (10 mL) was collected at 17:00 and urine was collected from 16:45–18:45.

Sample Processing

Urine was concentrated to 10% of its original volume and this portion was mixed with 9 volumes of 100% ethanol. The precipitate was centrifuged, the supernatant was evaporated to ≈10 mL, and the pH was adjusted to 8.0–9.0 with 1 M NaOH. The supernatant was applied to a 18 × 1 cm diameter Dowex-1X8-200-acetate column. The column was washed with 35 mL of water, the glucuronide eluted with 35 mL of 10 M acetic acid, and the acetic acid fraction was evaporated to dryness at 40–50°C. The residue was resuspended in 50 mL water and the pH was adjusted to 4.5–5.0.

Paracetamol glucuronide in this solution was derivatized to monoacetoneglucuronic lactone (MAGL) as previously described (14). Two thousand units of β-glucuronidase (*H. Pomatia,* Sigma Chemical, St. Louis, MO) were added and the solution was incubated at 45°C for 48 hr. The solution was then passed through 10 mL Dowex-50X8-200 H^+ ion-exchange resin and evaporated to complete dryness at 40°C, resulting in the conversion of free glucuronic acid to glucuronolactone. The lactone was converted to MAGL by stirring for 24 hr with 5 mL of anhydrous acetone and 0.1 mL concentrated H_2SO_4. The yellow solution was mixed with 5 mL water, the pH adjusted to between 4 and 5 with 0.5 M Na_2CO_3, and the solution evaporated to dryness at room temperature. MAGL was extracted from the salt products with 2–3 mL acetonitrile. For ^{13}C NMR analysis the acetonitrile supernatant was evaporated to dryness and the residue was resuspended in 0.6 mL of 20% deuterated acetonitrile.

NMR Spectroscopy

Proton-decoupled ^{13}C NMR spectra were obtained with an 11.75T Varian Unity spectrometer equipped with a 5-mm broadband probe. Spectra were acquired with a 60° pulse angle, an acquisition time of 2.5 sec, a sweep width of 25 kHz, and a pulse delay of 0.5 sec. The number of acquisitions ranged from 8,000–20,000 (6.7–16.7 hr). The summed free induction decays were processed with 0.1–0.2 Hz line broadening. All NMR spectra were analyzed using the curve-fitting routine supplied with the NUTS PC-based NMR spectral analysis program (Acorn NMR, Fremont CA). ^{13}C chemical shifts were referenced to the methyl carbon of nondeuterated acetonitrile at 0.3 ppm.

Metabolic Model

The metabolic model relating the formation of G6P ^{13}C-isotopomers from ^{13}C-triose phosphate precursors to metabolic exchange and dilution parameters is shown in Fig. 1. The model assumes negligible flux through the oxida-

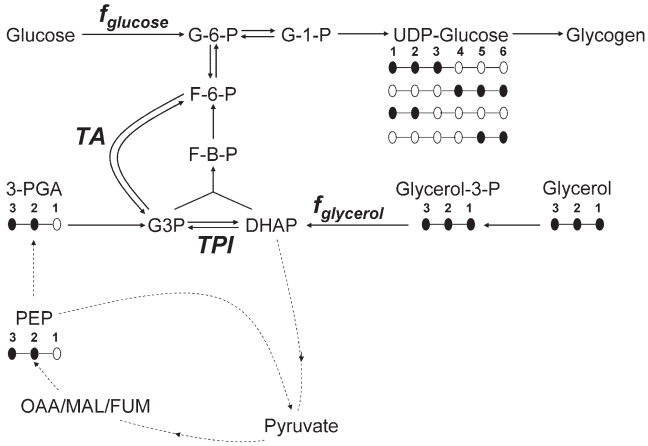

FIG. 1. Metabolic model for the metabolism of [1,2,3-$^{13}C_3$]glycerol to UDP-glucose (UDPG) during fed conditions featuring the four principal ^{13}C-isotopomers of UDPG that are formed under the experimental conditions. Hexose and triose isotopomers are represented by connected circles with each black circle representing ^{13}C and each white circle representing ^{12}C in the position of the molecule indicated by the number above. The conversion of [1,2,3-$^{13}C_3$]dihydroxyacetone phosphate (DHAP) to [2,3-$^{13}C_2$]3-phosphoglyceric acid (3-PGA) via pyruvate, C4 Krebs cycle metabolites (OAA/MAL/FUM), and the recycling of PEP to pyruvate, is represented by the dashed lines. The metabolic flux parameters shown in bold are as follows: $f_{glucose}$ = fraction of G6P directly derived from glucose; $f_{glycerol}$ = fraction of DHAP derived from glycerol; TPI = triose phosphate isomerase exchange; TA = transaldolase exchange.

tive branch of the PPP (15). The equations shown are specific to ^{13}C-isotopomers generated from the metabolism of [1,2,3-$^{13}C_3$]glycerol but they can be applied to glucuronide ^{13}C-isotopomers from other gluconeogenic ^{13}C-tracers such as [1,2,3-$^{13}C_3$]propionate or [3-^{13}C]lactate, or to glucuronide specific activity measurements from ^{14}C-gluconeogenic tracers. By formally redefining the source of unlabeled G6P as glycogen instead of glucose, the model can be applied to the fasted state. As illustrated in Fig. 1, [1,2,3-$^{13}C_3$]glycerol can be converted to G6P via a relatively direct pathway that involves entry into the triose phosphate pool to form [1,2,3-$^{13}C_3$]triose P followed by the synthesis of [1,2,3-$^{13}C_3$] or [4,5,6-$^{13}C_3$]hexose P via the aldolase reaction. At low enrichment levels (<5%), the probability of forming hexose P from two [1,2,3-$^{13}C_3$]triose P molecules is negligible. [1,2,3-$^{13}C_3$]Glycerol can also converted to G6P by an indirect route that involves the conversion of triose-P to pyruvate followed by the anaplerotic resynthesis of triose-P via pyruvate carboxylase and PEP carboxykinase. As a result of label randomization and pyruvate recycling via the Krebs cycle, the principal product of this indirect pathway is [2,3-$^{13}C_2$]3-PGA with only minor amounts of the [1,2,3-$^{13}C_3$]isotopomer.[2] On this basis, it is assumed that all [1,2,3-$^{13}C_3$]triose phosphate isotopomers originated from [1,2,3-$^{13}C_3$]glycerol-3-phosphate (G3P) and therefore entered the TPI reaction as [1,2,3-$^{13}C_3$]DHAP. Meanwhile, all [2,3-$^{13}C_2$]triose phosphate isotopomers are assumed to have originated from [2,3-$^{13}C_2$]3-PGA and therefore entered the TPI reaction as [2,3-$^{13}C_2$]GA3P. The isotopomers are assumed to be derived from a common pool of hepatic triose phosphates. The formation of G6P isotopomers from these two precursors are described by the following equations:

$$[1,2,3\text{-}^{13}C_3]G6P = 0.5 \times ([1,2,3\text{-}^{13}C_3]G3P \times f_{glycerol}) \times (1 + (1\text{-}TPI)) \times (1 - f_{glucose}) \quad [1]$$

$$[4,5,6\text{-}^{13}C_3]G6P = 0.5 \times ([1,2,3\text{-}^{13}C_3]G3P \times f_{glycerol}) \times TPI \times (1 - (f_{glucose} \times (1\text{-}TA))) \quad [2]$$

$$[1,2\text{-}^{13}C_2]G6P = 0.5 \times [2,3\text{-}^{13}C_2]3\text{-}PGA \times 0.5 \times (1 - (0.5 \times f_{glycerol} \times (1 + (1\text{-}TPI)))) \times (1 - f_{glucose}) \quad [3]$$

$$[5,6\text{-}^{13}C_2]G6P = 0.5 \times [2,3\text{-}^{13}C_2]3\text{-}PGA \times 0.5 \times (1 - (0.5 \times f_{glycerol} \times (1 - (1\text{-}TPI)))) \times (1 - (f_{glucose} \times (1\text{-}TA))) \quad [4]$$

where: $f_{glucose}$ = fraction of G6P directly derived from glucose; $f_{glycerol}$ = fraction of dihydroxyacetone phosphate derived from glycerol-3-phosphate; TPI = fraction of triose phosphate molecules that underwent triose phosphate isomerase exchange; TA = fraction of G6P molecules that underwent transaldolase exchange; G3P = glycerol-3-phosphate; 3-PGA = 3-phosphoglyceric acid.

The equations can be rearranged to relate the metabolic parameters to G6P isotopomer ratios:

$$[1,2,3\text{-}^{13}C_3]/[4,5,6\text{-}^{13}C_3]G6P = ((1 + (1\text{-}TPI)) \times (1 - f_{glucose}))/(TPI \times (1 - (f_{glucose} \times (1\text{-}TA)))) \quad [5]$$

$$[1,2\text{-}^{13}C_2]/[5,6\text{-}^{13}C_2]G6P = (1 - (0.5 \times f_{glycerol} \times (1 + (1\text{-}TPI))) \times (1 - f_{glucose}))/(1 - (0.5 \times f_{glycerol} \times (1 - (1\text{-}TPI))) \times (1 - (f_{glucose} \times (1\text{-}TA)))) \quad [6]$$

When exchange of GA3P with dihydroxyacetone phosphate (DHAP) is complete (TPI = 1.0), the two isotopomer ratios become equivalent and the equation simplifies as follows:

$$[1,2,3\text{-}^{13}C_3]/[4,5,6\text{-}^{13}C_3]G6P = [1,2\text{-}^{13}C_2]/[5,6\text{-}^{13}C_2]G6P = (1 - f_{glucose})/(1 - (f_{glucose} \times (1\text{-}TA))) \quad [7]$$

Hepatic G6P ^{13}C-isotopomer enrichments were quantified from the ^{13}C NMR multiplet signals of urinary glucuronide after derivatization to MAGL. ^{13}C-Enrichment of carbon 2 and the percent abundance of the [1,2,3-$^{13}C_3$]- and [1,2-$^{13}C_2$]isotopomers were determined from the carbon 2 multiplet of MAGL. As illustrated by Fig. 2, the multiplet component includes a central singlet signal (S), a quartet arising from ^{13}C-^{13}C coupling of carbon 2 with both carbons 1 and 3 (Q), and a doublet due to ^{13}C-^{13}C-coupling between carbons 1 and 2 (D). The contribution of each component is expressed as a fraction of the total multiplet area, arbitrarily given a value of 1.0. The singlet fraction (S) is assumed to be derived from natural abundance ^{13}C and is assigned an enrichment value of 1.11%. For all MAGL spectra this was confirmed by comparing the C2 and C5 singlet areas with those of the natural abundance MAGL methyl signals. In each case the singlet area was within 4% of the theoretical value (obtained from a human MAGL preparation where no ^{13}C-tracer was given). The Q and D components represent the contributions of [1,2,3-$^{13}C_3$]- and [1,2-$^{13}C_2$]G6P, respectively. On this basis the carbon 2 ^{13}C-enrichment and isotopomer abundances were calculated as follows.

$$\text{Total carbon 2 enrichment (\%)} = 1/S \times 1.11$$

$$\text{Excess carbon 2 enrichment (\%)} = \text{Total carbon 2 enrichment} - 1.11$$

$$[1,2,3\text{-}^{13}C_3]G6P \text{ enrichment} = Q/S \times 1.11$$

[2] [1,2,3-$^{13}C_3$]3-PGA is generated along with [2,3-$^{13}C_2$]3-PGA when [1,2,3-$^{13}C_3$]triose-P is converted to [1,2,3-$^{13}C_3$]pyruvate via glycolysis and resynthesized to triose-P via gluconeogenesis. Randomization by the Krebs cycle generates equal amounts of [1,2,3-$^{13}C_3$]- and [2,3-$^{13}C_2$]PEP and the recycling of PEP via pyruvate depletes the level of [1,2,3-$^{13}C_3$]- relative to [2,3-$^{13}C_2$]PEP (14). Given that the abundance of [1,2-$^{13}C_2$]G6P is about 20% that of [1,2,3-$^{13}C_3$]G6P, and assuming that pyruvate cycling is inactive, the maximal contribution of [1,2,3-$^{13}C_3$]3-PGA to the total [1,2,3-$^{13}C_3$]triose-P pool is ≈20%. If pyruvate cycling activity is the same as that reported for overnight fasting (15), the contribution falls to ≈8%.

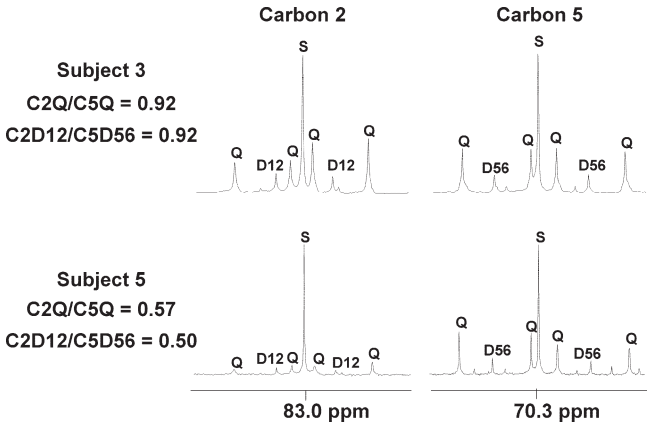

FIG. 2. ^{13}C NMR signals of carbons 2 and 5 from the monoacetone glucuronic lactone derivative of paracetamol glucuronide from subjects 3 and 5. The carbon 2 and 5 ^{13}C-resonances are shown in expanded view and their multiplet components are labeled as follows: For carbon 2; S = natural abundance singlet, Q = quartet signal from [1,2,3-$^{13}C_3$]glucuronide and D = doublet signal from [1,2-$^{13}C_2$]glucuronide. For carbon 5; S = natural abundance singlet, Q = quartet signal from [4,5,6-$^{13}C_3$]glucuronide and D = doublet signal from [5,6-$^{13}C_2$]glucuronide. The ratio of [1,2,3-$^{13}C_3$]glucuronide to [4,5,6-$^{13}C_3$]glucuronide (represented by C2Q/C5Q) and [1,2-$^{13}C_2$]glucuronide to [5,6-$^{13}C_2$]glucuronide (represented by D12/D56) are also shown for both subjects.

$$[1,2\text{-}^{13}C_2]\text{G6P enrichment} = D/S \times 1.11$$

Analogous equations were derived for G6P carbon 5 enrichment and isotopomer abundances by analysis of the MAGL carbon 5 multiplet:

$$\text{Total carbon 5 enrichment (\%)} = 1/S \times 1.11$$

$$\text{Excess carbon 5 enrichment (\%)} = \text{Total carbon 5 enrichment} - 1.11$$

$$[4,5,6\text{-}^{13}C_3]\text{G6P enrichment} = Q/S \times 1.11$$

$$[5,6\text{-}^{13}C_2]\text{G6P enrichment} = D/S \times 1.11$$

The difference in isotopomer enrichment levels between carbons 1, 2, 3 and 4, 5, 6 of glucuronide were analyzed by the paired 2-tailed Student's *t*-test. Differences were considered significant at $P < 0.05$.

RESULTS

Model Predictions

The metabolic model relates TA and TPI exchanges to the ^{13}C-isotopomer enrichment of the G3P triose moieties from ^{13}C-enriched gluconeogenic precursors. These precursors can enter the triose phosphate isomerase reaction as DHAP (i.e., ^{13}C-glycerol) or as GA3P (i.e., ^{13}C-lactate). When TPI exchange is incomplete the triose halves of G6P are enriched to unequal levels from either precursor substrate. With tracers that enter as DHAP (for example [1,2,3-$^{13}C_3$]glycerol), carbons 1, 2, and 3 of G6P will have higher ^{13}C-enrichment than carbons 4, 5, and 6. With gluconeogenic tracers that enter as GA3P prior to TPI exchange (i.e., ^{13}C-lactate), the G6P enrichment pattern is reversed, with carbons 4, 5, and 6 being more enriched than carbons 1, 2, and 3. Under postabsorptive and fed conditions, the contribution of glycerol carbons to total gluconeogenic flux is small (5–10%). Therefore, for the simulated data shown in Table 1 we assumed that 10% of DHAP flux was derived from glycerol-3-P. Under these conditions, the effect of incomplete TPI exchange on the inequality of ^{13}C-enrichment between the triose halves of G6P is relatively minor with enriched GA3P precursors. In this study, GA3P is enriched from the indirect metabolism of [1,2,3-13C3]glycerol and is represented by [1,2]- and [5,6-13C2]G6P. However, other tracers that are metabolized via the Krebs cycle, such as 13C-lactate, will also generate 13C-enriched GA3P. For example, when TPI exchange is 80% complete the difference in ^{13}C-enrichment levels between the triose moieties of G6P is only 2% (see Table 1). However, for DHAP precursors the ^{13}C-enrichment distribution between the triose halves of G6P is far more sensitive to the level of TPI exchange. As shown in Table 1, a TPI exchange that is 80% complete results in a 50% higher ^{13}C-enrichment in the 1,2,3-triose compared to the 4,5,6-triose moiety of G6P. The addition of unlabeled G6P from glucose will systematically dilute the ^{13}C-enrichment levels but it has no effect on the relative ^{13}C-enrichments of the G6P triose halves. When TPI exchange is complete the triose halves of G6P are equivalently enriched regardless of the ^{13}C-tracer source.

TA exchange modifies the ^{13}C-enrichment distribution by exchanging an unlabeled carbon 4, 5, 6-moiety of F6P with ^{13}C-enriched GA3P. Therefore, regardless of whether the tracer originated via GA3P or DHAP, the effect of TA exchange is to increase the enrichment in carbons 4, 5, and 6 of G6P relative to carbons 1, 2, and 3. For a given level of TA activity, the inequality between the ^{13}C-enrichment of the G6P triose halves becomes greater as the fraction of G6P derived from unlabeled hexose sources ($f_{glucose}$) is increased.

Experimental Data

The MAGL derivative of urinary paracetamol glucuronide provided high-resolution ^{13}C NMR spectra of the carbon 2 and 5 ^{13}C-isotopomer signals of the glucuronide moiety (14), as illustrated by the examples shown in Fig. 2. The [1,2,3-$^{13}C_3$]- and [4,5,6-$^{13}C_3$]glucuronide isotopomer pair derived from the incorporation of [1,2,3-$^{13}C_3$]glycerol into G6P via glycerol kinase and triose phosphate intermediates are resolved as spin-spin coupled quartets within the carbon 2 and 5 ^{13}C NMR signals. Enrichment from [1,2,3-$^{13}C_3$]glucuronide was always less than that of [4,5,6-$^{13}C_3$]glucuronide. This isotopomer distribution is opposite to that predicted from incomplete TPI exchange (see Table 2) but is consistent with TA activity. The ^{13}C NMR signals of [1,2-$^{13}C_2$]- and [5,6-$^{13}C_2$]glucuronide, which represent triose phosphate ^{13}C-isotopomers derived via PEP and the Krebs cycle, were also well resolved in the spectra, albeit with low intensities. The observation of corresponding [2,3-$^{13}C_2$]glutamine ^{13}C-isotopomer signals from urinary phenylacetylglutamine obtained from each subject is con-

Table 1
Theoretical G6P ^{13}C-Isotopomer Ratios of [1,2,3-13C3]Glycerol Metabolism Derived from the Metabolic Flux Equations Using the Metabolic Flux Parameter Values Shown. The [1,2]- and [5,6-13C2]G6P Isotopomers Represent Metabolism of [1,2,3-13C3]Glycerol via Krebs Cycle and Glyceraldehyde-3-Phosphate Intermediates.

^{13}C-Isotopomer ratios of G6P		Metabolic flux parameters			
[1,2,3-$^{13}C_3$]/[4,5,6-$^{13}C_3$]G6P	[1,2-$^{13}C_2$]/[5,6-$^{13}C_2$]G6P	$f_{glycerol}$	TPI	$f_{glucose}$	TA
1.00	1.00	0.1	1.0	0.0	0.0
1.50	0.98	0.1	0.80	0.0	0.0
1.00	1.00	0.1	1.00	0.5	0.0
1.50	0.98	0.1	0.80	0.5	0.0
0.83	0.83	0.1	1.00	0.5	0.2
1.25	0.82	0.1	0.80	0.5	0.2
1.07	0.71	0.1	0.80	0.5	0.4
0.95	0.71	0.1	0.95	0.5	0.4
0.73	0.71	0.1	0.99	0.5	0.4
0.71	0.71	0.1	1.00	0.5	0.4

sistent with the hepatic Krebs cycle origins of [1,2-$^{13}C_2$]- and [5,6-$^{13}C_2$]glucuronide (data not shown). Overall, the ratio of [1,2-$^{13}C_2$]- to [5,6-$^{13}C_2$]glucuronide was in reasonably close agreement with that of [1,2,3-$^{13}C_3$]- to [4,5,6-$^{13}C_3$]glucuronide. Because of the low D12 and D56 signal intensities (a signal-to-noise ratio of 10:1 for the D12 signals of Subject 5), the [1,2-$^{13}C_2$]- to [5,6-$^{13}C_2$]glucuronide ratio is associated with a higher level of uncertainty than that of [1,2,3-$^{13}C_3$]- to [4,5,6-$^{13}C_3$]glucuronide.

As indicated by the simulated data of Table 1, the concordance of these isotopomer ratios is consistent with TPI exchange being ≈99% complete. Under these conditions the simplified equation (Eq. [7]) can provide reasonable estimates of TA exchange from the glucuronide ^{13}C-isotopomer ratios for a given fraction of direct pathway contribution ($f_{glucose}$) to G6P synthesis. For healthy subjects under fed conditions, 50–70% of hepatic G6P is derived directly from glucose (7,10,18). Assuming a direct pathway contribution of 60%, the fraction of G6P undergoing TA exchange was estimated for each subject, as shown in Table 3. In addition, we calculated the apparent direct and indirect pathway contributions that would be estimated with glucose tracers that are diluted by TA exchange ([6-^{14}C]- and [5-^{3}H]glucose).

The data indicate that for three of the subjects the extent of TA exchange and its effects on direct and indirect pathway estimates was relatively small. However, the remaining two subjects had substantial TA exchange activities, resulting in a sizeable overestimation of the indirect pathway contribution to UDP-glucose synthesis. As shown by the examples in Fig. 2, the smaller intensity of the carbon 2 multiplets relative to those of carbon 5 is quite sensitive to the fraction of G6P undergoing TA activity. The unequal intensities of the carbon 2 and 5 multiplets were also accompanied by similar differences between the multiplets of glucuronide carbons 3 and 4 (data not shown).[3]

DISCUSSION

The labeling distribution of glucuronide from gluconeogenic tracers is influenced by both TPI and TA exchanges. Depending on the source of the gluconeogenic tracer, the effect of incomplete TPI exchange on the ^{13}C-enrichment distribution between the triose halves can either augment or oppose that of TA. Therefore, in order to evaluate the extent of TA activity the contribution of incomplete TPI exchange to the enrichment distribution of glucuronide has to be considered. In humans the formation of glucuronide or glucose with unequal labeling of the triose halves have been reported with several different ^{13}C-and ^{14}C-gluconeogenic tracers (19–21). Most of these measurements were obtained after extended fasting when the fraction of G6P derived from glycogenolysis is small. Under these conditions the glucuronide or glucose labeling distribution is insensitive to TA activity but it is influenced by incomplete TPI exchange. The distribution of radioactivity from [2-^{14}C]glycerol and [1-^{14}C]lactate in the triose halves of glucuronide was quantified in 36-hr fasted humans (20). The specific activity from [2-^{14}C]glycerol was ≈20% higher in C2 compared to C5 of glucuronide, while the specific activity from [1-^{14}C]lactate was ≈10% higher in C4 compared to C3. These observations are consistent with hepatic TPI exchange being ≈90% complete. In individuals that were fasted for 60 hr and infused with ^{14}C-propionate or ^{14}C-acetate, there was essentially equal distribution of label between the triose moieties of plasma glucose, indicating near complete TPI exchange (8,21). However, when [3-^{14}C]lactate was infused under fed conditions the specific activities of carbons 5 and 6 of glucose were 1.4–1.6 times greater than those of carbons 1 and 2 and this was attributed to a combination of TA activity and incomplete TPI exchange (8). In light of our current findings and the previously cited reports of near complete TPI exchange in human liver, we conclude that the unequal specific activity distributions in the triose halves of glucose reported by Magnusson et al. (8) are largely attributable to TA exchange. We applied the specific activity ratios of glucose carbon 1 to carbon 6 and carbon 2 to carbon 5 to our model using the same assumptions as for our ^{13}C-isotopomer data (i.e., 60% direct pathway contribution and complete TPI exchange). This analysis revealed that in the study of Magnusson et al. 33% of hepatic G6P had participated in TA exchange.

The isotopomer analysis relies on the assumption that flux through the oxidative portion of the PPP is negligible

[3] [2,3-$^{13}C_2$]Oxaloacetate is the main source of both hepatic [2,3-$^{13}C_2$]triose-P and [2,3-$^{13}C_2$]glutamine.

Table 2
G6P ^{13}C-Isotopomer Ratios Derived from ^{13}C-NMR Isotopomer Analysis of Urinary Glucuronide of Five Healthy, Fed Subjects Following Ingestion of [1,2,3-$^{13}C_3$]Glycerol and Paracetamol

Subject	Carbon 2 ^{13}C-enrichment and isotopomer distribution of G6P			Carbon 5 ^{13}C-enrichment and isotopomer distribution of G6P			Carbon 2 to carbon 5 isotopomer ratios of G6P	
	Percent excess ^{13}C-enrichment	Percent [1,2,3-$^{13}C_3$]G6P	Percent [1,2-$^{13}C_2$]G6P	Percent Excess ^{13}C-enrichment	Percent [4,5,6-$^{13}C_3$]G6P	Percent [5,6-$^{13}C_2$]G6P	$\frac{[1,2,3\text{-}^{13}C_3]}{[4,5,6^{13}C_3]}$	$\frac{[1,2\text{-}^{13}C_2]}{[5,6\text{-}^{13}C_2]}$
1	1.91	1.55	0.30	2.17	1.69	0.36	0.92	0.85
2	2.03	1.55	0.35	2.42	1.92	0.39	0.81	0.88
3	2.45	1.98	0.36	2.68	2.16	0.39	0.92	0.92
4	0.80	0.54	0.24	1.48	1.06	0.34	0.51	0.71
5	1.07	0.86	0.16	1.96	1.52	0.32	0.57	0.50
Mean	1.65	1.30	0.28	2.14	1.67	0.36	0.75	0.77
SD	0.68	0.57[a]	0.08[b]	0.46	0.42	0.03	0.19	0.17

[a]Significantly less abundant than [4,5,6-$^{13}C_3$]glucuronide, $P < 0.05$. [b]Significantly less abundant than [5,6-$^{13}C_2$]glucuronide, $P < 0.05$.

in comparison to gluconeogenic fluxes (15). The presence of oxidative PPP flux would have a significant effect on the ^{13}C-isotopomer distributions of G6P. For example, the loss of carbon 1 following the conversion of G6P to ribose-5-P would initially generate [1,2-$^{13}C_2$] and [2-^{13}C]ribose-5-P from [1,2,3-$^{13}C_3$]- and [1,2-$^{13}C_2$]G6P, respectively. One likely consequence is that PPP flux would significantly alter the isotopomer ratio of [1,2-$^{13}C_2$]/[1,2,3-$^{13}C_3$]G-6-P while that of [5,6-$^{13}C_2$]/[4,5,6-$^{13}C_3$]G6P would be relatively unaffected. The fact that the experimental [1,2-$^{13}C_2$]/[1,2,3-$^{13}C_3$]G-6-P and [5,6-$^{13}C_2$]/[4,5,6-$^{13}C_3$]G6P ratios were equal, as seen in Table 2, is consistent with minimal PPP flux. In two of the subjects the ratio of [1,2-$^{13}C_2$]/[5,6-$^{13}C_2$]G6P was higher than that of [1,2,3-$^{13}C_3$]/[4,5,6-$^{13}C_3$]G6P. In the metabolic model, the ratio of [1,2-$^{13}C_2$]/[5,6-$^{13}C_2$]G6P can approach but not exceed that of [1,2,3-$^{13}C_3$]/[4,5,6-$^{13}C_3$]G6P. Our experimental data may be a consequence of the high uncertainty in quantifying the small [1,2-$^{13}C_2$]- and [5,6-$^{13}C_2$]G6P NMR signals. Alternatively, these isotopomer distributions may be real, therefore revealing a discrepancy between the metabolic model and in situ fluxes. A key assumption of the model is that all G6P isotopomers originate from a common pool of gluconeogenic metabolites, but it is well known that there is considerable metabolic heterogeneity between periportal and perivenal hepatocytes, particularly regarding glycerol metabolism. Glycerol is avidly metabolized by periportal cells, hence the distribution of the two primary G6P isotopomers ([1,2,3-$^{13}C_3$] and [4,5,6-$^{13}C_3$]G6P) may be weighted toward periportal TA activity. In comparison, the [1,2-$^{13}C_2$] and [5,6-$^{13}C_2$]G6P isotopomer pair are derived via pyruvate/lactate and therefore may reflect TA activity from a broader region of the hepatic lobule, given the more homogenous hepatic uptake of lactate/pyruvate compared to glycerol (20). If TA activity in the pericentral/perivenous region was lower than that of periportal cells, this would provide an explanation for the [1,2-$^{13}C_2$]/[5,6-$^{13}C_2$]G6P ratio being higher than that of [1,2,3-$^{13}C_3$]/[4,5,6-$^{13}C_3$]G6P.

The presence of TA activity has important implications for quantifying the gluconeogenic contribution to human hepatic G6P synthesis with either stable-isotope or radioactive tracers, at least under fed conditions. Tracers such as [5-^{3}H]glucose or [6-^{13}C]glucose undergo dilution as a result of TA activity resulting in overestimates of the indirect pathway contribution to G6P synthesis. TA exchange does not result in the dilution of [1-^{13}C]- or [1-^{14}C]glucose at the level of G6P; therefore, estimates of direct and indirect pathway fractions with these tracers will not be affected. With the $^{2}H_2O$ measurement of direct and indirect pathway contributions (7), the fraction of G6P derived from the indirect pathway is quantified as the ratio of glucuronide hydrogen 5 enrichment relative to that of body water. TA activity contributes to the enrichment of

Table 3
Estimates of the Fraction of G6P Undergoing TA Exchange for the Five Subjects

Subject	Percentage of G6P that underwent TA exchange	Apparent percentage of UDP-glucose derived from direct pathway (assuming a theoretical value of 60%)	Apparent percentage of UDP-glucose derived from indirect pathway (assuming a theoretical value of 40%)
1	8	55	45
2	12	53	47
3	5	57	43
4	43	34	66
5	57	26	74
Mean (± SD)	25 ± 23	45 ± 14	55 ± 14

TA was solved from Eq. [7] using the mean C2 and C5 isotopomer ratios and assuming a direct pathway fraction of 60% ($f_{glucose} = 0.6$) and indirect pathway fraction of 40%. Triose phosphate isomerase exchange is assumed to be complete (TPI = 1.0). Also shown are the apparent direct and indirect pathway percentage contributions to UDP-glucose flux, and the deviations from the theoretical values that would be obtained with tracers such as [5-^{3}H]- or [6-^{13}C]glucose.

hydrogen 5, resulting in an overestimate of the indirect pathway fraction (7).

In summary, transaldolase exchange is active in human liver and it may result in significant overestimates of hepatic gluconeogenic activity with ^2H_2O, gluconeogenic carbon tracers, or certain glucose tracers at least in the fed state. Our data indicate that the unequal enrichment of the triose moieties of G6P from ^{13}C gluconeogenic tracers is almost entirely attributable to transaldolase activity and that transaldolase exchange can be quantified from the relative ^{13}C-enrichments of the G6P triose halves. With gluconeogenic carbon tracers such as ^{13}C-glycerol or ^{13}C-lactate, this information is inherent in the ^{13}C-enrichment distribution of plasma glucose or urinary glucuronide, and hence in principle it could be used to correct for transaldolase activity.

REFERENCES

1. Gastaldelli A, Baldi S, Pettiti M, Toschi E, Camastra S, Natali A, Landau BR, Ferrannini E. Influence of obesity and type 2 diabetes on gluconeogenesis and glucose output in humans: a quantitative study. Diabetes 2000;49:1367–1373.
2. Magnusson I, Rothman DL, Katz LD, Shulman RG, Shulman GI. Increased rate of gluconeogenesis in type II diabetes mellitus. A ^{13}C nuclear magnetic resonance study. J Clin Invest 1992;90:1323–1327.
3. Bugianesi E, Kalhan S, Burkett E, Marchesini G, McCullough A. Quantification of gluconeogenesis in cirrhosis: response to glucagon. Gastroenterology. 1998;115:1530–1540.
4. Dekker E, Romijn JA, Ekberg K, Wahren J, Van TH, Ackermans MT, Thuy LT, Chandramouli V, Kager PA, Landau BR, Sauerwein HP. Glucose production and gluconeogenesis in adults with uncomplicated falciparum malaria. Am J Physiol 1997;272:E1059–E1064.
5. Hellerstein MK, Greenblatt DJ, Munro HN. Glycoconjugates as noninvasive probes of intrahepatic metabolism — pathways of glucose entry into compartmentalized hepatic UDP-glucose pools during glycogen accumulation. Proc Natl Acad Sci U S A 1986;83:7044–7048.
6. Magnusson I, Chandramouli V, Schumann WC, Kumaran K, Wahren J, Landau BR. Quantitation of the pathways of hepatic glycogen formation on ingesting a glucose load. J Clin Invest 1987;80:1748–1754.
7. Jones JG, Fagulha A, Barosa C, Bastos M, Barros L, Baptista C, Caldeira MM, Carvalheiro, M. Noninvasive assessment of hepatic glycogen kinetics before and after a breakfast meal with deuterated water and acetaminophen. Diabetes 2006;55:2294–2300.
8. Magnusson I, Schumann WC, Bartsch GE, Chandramouli V, Kumaran K, Wahren J, Landau BR. Noninvasive tracing of Krebs cycle metabolism in liver. J Biol Chem 1991;266:6975–6984.
9. Landau BR, Wahren J, Chandramouli V, Schumann WC, Ekberg K, Kalhan SC. Contributions of gluconeogenesis to glucose production in the fasted state. J Clin Invest 1996;98:378–385.
10. Stingl H, Chandramouli V, Schumann WC, Brehm A, Nowotny P, Waldhausl W, Landau BR, Roden M. Changes in hepatic glycogen cycling during a glucose load in healthy humans. Diabetologia 2006; 49:360–368.
11. Ljungdahl L, Wood HG, Couri D, Racker E. Formation of unequally labelled fructose-6-phosphate by an exchange reaction catalyzed by transaldolase. J Biol Chem 1961;236:1622–1625.
12. Landau BR, Bartsch GE. Estimations of pathway contributions to glucose metabolism and the transaldolase reactions. J Biol Chem 1966;241: 741–749.
13. Flanigan I, Collins JG, Arora KK, Macleod JK, Williams JF. Exchange reactions catalyzed by group transferring enzymes oppose the quantification and the unravelling of the identity of the pentose phosphate pathway. Eur J Biochem 1993;213:477–485.
14. Jones JG, Barosa C, Gomes F, Mendes AC, Delgado TC, Diogo L, Garcia P, Bastos M, Barros L, Fagulha A, Baptista C, Carvalheiro M, Caldeira MM. NMR derivatives for quantification of H-2 and C-13-enrichment of human glucuronide from metabolic tracers. J Carb Chem 2006;25:203–217.
15. Magnusson I, Chandramouli V, Schumann WC, Kumaran K, Wahren J, Landau BR. Pentose pathway in human liver. Proc Natl Acad Sci U S A 1988;85:4682–4685.
16. Jones JG, Naidoo R, Sherry AD, Jeffrey FMH, Cottam GL, Malloy CR. Measurement of gluconeogenesis and pyruvate recycling in the rat liver: a simple analysis of glucose and glutamate isotopomers during metabolism of [1,2,3-$^{13}C_3$]propionate. FEBS Lett 1997;412:131–137.
17. Jones JG, Solomon M.A, Cole SM, Sherry AD, Malloy CR. An integrated ^2H and ^{13}C NMR study of gluconeogenesis and TCA cycle flux in humans. Am J Physiol 2001;281:E848–E851.
18. Bischof MG, Bernroider E, Krssak M, Krebs M, Stingl H, Nowotny P, Yu CL, Shulman GI, Waldhausl W, Roden M. Hepatic glycogen metabolism in type 1 diabetes after long-term near normoglycemia. Diabetes 2002; 51:49–54.
19. Jones JG, Solomon MA, Sherry AD, Jeffrey FMH, Malloy CR. ^{13}C NMR measurements of human gluconeogenic fluxes after ingestion of [U-^{13}C]propionate, phenylacetate, and acetaminophen. Am J Physiol 1998;275:E843–E852.
20. Ekberg K, Chandramouli V, Kumaran K, Schumann WC, Wahren J, Landau BR. Gluconeogenesis and glucuronidation in liver in vivo and the heterogeneity of hepatocyte function. J Biol Chem 1995;270:21715–21717.
21. Landau BR, Schumann WC, Chandramouli V, Magnusson I, Kumaran K, Wahren J. ^{14}C-labeled propionate metabolism in vivo and estimates of hepatic gluconeogenesis relative to Krebs cycle flux. Am J Physiol 1993;265:E636–E647.